Astron. Astrophys. 295, 403–412 (1995)

ASTRONOMY AND ASTROPHYSICS

SN 1993J in M 81: optical photometry and spectrophotometry during the first two months

T.P. Prabhu[1], Y.D. Mayya[1⋆], K.P. Singh[2], N. Kameswara Rao[1], K.K. Ghosh[3], M.V. Mekkaden[1], A.K. Pati[1], A.V. Raveendran[1], B.E. Reddy[1], R. Sagar[1], A. Subramaniam[1], and R. Surendiranath[1]

[1] Indian Institute of Astrophysics, Bangalore 560034, India
[2] Tata Institute of Fundamental Research, Homi Bhabha Road, Colaba, Bombay 400005, India
[3] Vainu Bappu Observatory, Kavalur, Alangayam 635701, Tamil Nadu, India

Received 25 July 1994 / Accepted 9 September 1994

Abstract. CCD photometric and spectrophotometric data on the type IIb supernova 1993J in M 81 (NGC 3031) obtained from Vainu Bappu Observatory, Kavalur, during the first two months since the outburst are reported. The evolution of the spectrum is described. The evolution of the velocity of P-Cygni absorption dips due to different lines is presented. The photospheric temperature and radius are determined using blackbody fits to $BVRIJHK$ photometry after correcting for interstellar extinction and contribution to the band by the net line emission. The evolution of photospheric radius implies a density variation in the progenitor $\rho \propto r^{-n}$ with $n = 5 - 6$ during the rise to the second maximum reducing to $n = 2$ soon after. These values are comparable to the corresponding values for SN1987A. An application of the expanding photosphere method yields a distance of 2.2 – 5.1 Mpc for the range of $E(B-V) = 0.08 - 0.32$, and the atmospheric dilution factor $\zeta = 0 - 0.4$. The distance estimates with the assumption of low reddening and low dilution as well as moderate reddening and moderate dilution are both consistent with the HST Cepheid distance to M 81 (3.6 ± 0.3 Mpc).

Key words: supernovae: individual, SN 1993J – stars: distances – galaxies: individual, M 81 (NGC 3031)

1. Introduction

The photometric and spectroscopic diversity of supernovae (SN) is increasingly being recognized during the last decade, largely due to the peculiarities noted in recent SN such as SN 1983N in M 83 (type Ib), SN 1987A in the Large Magellanic Cloud (subluminous type II with a blue supergiant progenitor), and SN 1987K in NGC 4651 (type IIb) (Filippenko 1988, 1991; Harkness & Wheeler 1990). This suggests that there could be a diversity in the properties of progenitors as well. It is thus important to study individual SN in detail in order to understand the physical phenomena involved. The discovery of SN 1993J in the nearby galaxy M 81 by F. Garcia (Ripero 1993) on 1993 March 28 provided such an opportunity since it reached a maximum brightness of $V \sim 10$. Though it started as type II, as time progressed it became evident that the SN was peculiar with a good resemblance to SN 1987K which had changed from type II at maximum to type Ib during nebular stage. The transition was better observed in the case of SN 1993J (Filippenko et al. 1993). SN 1987K has earlier been identified with the explosion of a 10–20$M_\odot$ progenitor soon after losing most of its envelope to a companion (Woosley et al. 1987; Woosley 1991).

SN 1993J has been observed well in the optical, infrared and radio bands by most of the observatories in the northern hemisphere, and also in the satellite ultraviolet, X-ray and γ-ray regions. A review of early observations and interpretation is given by Wheeler & Filippenko (1993). Spectrophotometric and photometric data for the first 50 days has been presented by Schmidt et al. 1993) who derived a distance of 2.6 ± 0.4 Mpc using expanding photosphere method. An application of the method in the radio region by Bartel et al. (1994) yielded a distance of 4.0 ± 0.6 Mpc, consistent with the Hubble Space Telescope measurement of 3.63 ± 0.34 Mpc (Freedman et al. 1994) for M 81 using Cepheid variables. The distance to M 81 has been determined using several independent techniques such as Cepheid light curves, Tully-Fisher relation, brightest stars, H II regions, planetary nebula luminosity function, and surface brightness fluctuations. The estimates generally lie in the range 3.0–3.7 Mpc (cf. Freedman et al. 1994).

Recently, Lewis et al. (1994) have published detailed optical observations of SN 1993J during the first 4 months, while Richmond et al. (1994) presented extensive $UBVRI$ photometric data. We present here photometric and spectrophotometric re-

Send offprint requests to: T.P. Prabhu
⋆ Present address: Infrared Astronomy Group, Tata Institute of Fundamental Research, Homi Bhabha Road, Colaba, Bombay 400005, India.

sults on SN 1993J based on observations obtained with the 1-m and 2.3-m telescopes at the Vainu Bappu Observatory (VBO), Kavalur, betweeen 1993 April 1 and May 23. The photometric observations are presented in Sect. 2 and the spectrophotometric observations in Sect. 3. The photospheric evolution is described in Sect. 4 and expanding photosphere method is applied to estimate the distance to the supernova. The conclusions are summarized in Sect. 5.

2. Photometry

CCD images of the region around SN 1993J were obtained on a total of 11 nights between 1993 April 14 and May 23 at the prime focus of the 2.3-m Vainu Bappu telescope. Two CCD cameras — one belonging to IIA and the other belonging to TIFR/IUCAA — were employed both of which have nearly identical GEC 8603 CCD chips of format 385 × 578 pixels of 23μm size. The image scale corresponds to 0.6 arcsec per pixel and the field is $\sim 4 \times 6$ arcmin^2. Images were recorded generally in BVR bands and on two nights also in the I band. The systems are calibrated to Cousins $BVRI$ bands by Anupama et al. (1994) and Mayya (1993).

The photometry was carried out differentially with respect to star B (Corwin 1993) as comparison star and star A as the check star. (see Richmond et al. 1994 for an identification chart.) The magnitudes were measured with an aperture of radius 15 pixels (8 arcsec) and the sky background was taken from an annulus of 10 pixels width and inner radius of 25 pixels. The image size (full width at half maximum) ranged from 3–5 pixels (~2–3 arcsec). APPHOT package of IRAF[1] was used for the measurements. Zero-points were computed on each night with star B as the standard. Colour corrections needed were negligible during the early days when the colours of SN were similar to those of star B, but became very significant as the SN became progressively redder. The results are listed in Table 1. The quoted errors for star B are the rms of zero-points which indicate the variation in the atmospheric transmission on different nights. In the case of star A, the errors are rms of derived magnitudes, which represent well the errors in the photometry.

The photometry from VBO compares well with other available photometry (cf. Prabhu 1994). A comparison with the published photometry of Schmidt et al. 1993) shows that the difference between our BVR magnitudes and those from Schmidt et al. are 0.0 ± 0.05, -0.01 ± 0.02 and -0.05 ± 0.01 during 1993 April. Similar numbers for La Palma results presented by Richmond et al. (1994) are 0.03 ± 0.05, -0.01 ± 0.04 and -0.04 ± 0.03; for Kitt Peak 0.03 ± 0.04, 0.02 ± 0.01 and -0.05 ± 0.02; for Leuschner 50cm 0.10 ± 0.05, 0.07 ± 0.03 and -0.01 ± 0.03; and for Leuschner 76cm 0.09 ± 0.05, 0.07 ± 0.02 and 0.03 ± 0.03. The La Palma data has been independently reduced by Richmond et al. (1994) as well as Lewis et al. (1994) and there are systematic differences of 0.01–0.03 between the two results. We conclude that the Leuschner results are of relatively poorer quality (as is apparent from the colour plots of Richmond et al.); that systematic errors of up to 0.03 mag are possible between different observations; and that our R measures are likely to be 0.04–0.05 mag brighter than other data due to systematic errors. The two I measurements we have are 0.06–0.07 mag fainter compared to La Palma and Kitt Peak data. These differences are very likely originating from the small differences in filter and detector response which do not get fully corrected for spectra that are so much different from those of standard stars. The May 1994 results of Richmond et al. and Lewis et al. differ considerably in the case of La Palma data. Our measurements are slightly fainter than the two, but are much closer to Lewis et al. results than the Richmond et al. results. Similar comments are valid also for the photometric results presented by van Driel et al. (1993) and Benston et al. (1994) for the same period. While systematic errors of few tenths of magnitude seem possible between different measurements, it may be that some of the significant deviations from the mean, for example on April 17.65 and 22.69 in our data, arise due to real variations of up to 0.1 mag in less than 24 hours. Such variations can be monitored only with a whole earth coverage.

Pre-discovery and subsequent observations show that SN 1993J steadily brightened from a magnitude > 17 on 1993 March 27.9 to $V = 10.7$ on March 30.3 (Wheeler et al. 1993). We will adopt the date of outburst as 1993 March 28.1 in the following. The initial rise in the light curves was followed by a sharp drop to $V = 11.9$ on April 5. The SN then brightened

Table 1. VBO photometry of SN 1993J.

Date 1993	Day[1]	V	$B-V$	$V-R$	V-I
April 14.68	17.58	10.957	0.521	0.390	
April 15.67	18.57	10.898	0.497	0.397	
April 16.68	19.58	10.865	0.530	0.425	
April 17.65	20.55	10.869	0.630	0.406	
April 18.62	21.52	10.847	0.576	0.396	
April 19.62	22.52	10.885	0.675	0.426	
April 21.61	24.51	10.976	0.780	0.473	0.520
April 22.59	25.49	11.049	0.876	0.475	
April 24.60	27.50	11.267	0.935	0.557	0.637
May 21.61	54.51	12.473	1.269	0.686	
May 23.64	56.54	12.538	1.392	0.707	
Star B[2]	11.900 ±0.018	0.500 ±0.023	0.300 ±0.008	0.600 ±0.008	
Star A[3]	11.407 ±0.016	0.539 ±0.021	0.306 ±0.022	0.604 ±0.010	

1. Day 0 = March 28.1
2. Comparison star. Magnitudes are the assumed ones whereas the errors are rms of zero point corrections on different nights.
3. Check star. Derived magnitudes and errors.

[1] IRAF is distributed by the National Optical Astronomy Observatories, which is operated by the Association of Universities, Inc. (AURA) under cooperative agreement with the National Science Foundation.

slowly to $V = 10.8$ till April 18 and declined thereafter. The colours turned redder steadily after the secondary maximum on April 18. This behaviour resembles the light curve of SN 1987A though the latter was about 1.4 mag fainter in absolute brightness in V band, and reached the second peak $\sim$ 90 days since the outburst compared to only $\sim$ 20 days in the case of SN 1993J.

The models of supernovae constructed soon after the outburst of SN 1987A qualitatively explain such light curves and have hence been refined since the outburst of SN 1993J (see, e.g. Nomoto et al. 1993; Podsiadlowski et al. 1993; Ray et al. 1993; Swartz et al. 1993; Wheeler et al. 1993; Woosley et al. 1994; Woosley et al. 1994). It would appear that a 10–20$M_\odot$ progenitor had lost all but a few tenths of $M_\odot$ of envelope to a companion leaving behind a helium core of $\sim 3M_\odot$ and a helium-rich H+He mantle just before the explosion. Approximately $0.05-0.1M_\odot$ of radioactive nickel was produced during the explosion. The type IIb SN differs from type Ib only in that the latter does not have any envelope. The faster evolution of SN 1993J compared to SN 1987A to the secondary maximum was due to the lower envelope mass (see Höflich et al. 1993 for a model that differs significantly from others mentioned above).

Table 2. Journal of spectroscopic observations of SN 1993J.

Date 1993	Day	Wavelength range (Å)	Dispersion[1] Å/pixel	Tel. m
April 1.694	4.594	6150–6900	1.4	1.0
April 3.667	6.567	5200–8300	5.5	1.0
April 6.601	9.501	4350–6850	4.5	2.3
April 7.734	10.634	4370–6840	4.5	2.3
April 8.644	11.544	4420–6840	4.5	2.3
April 13.625	16.525	3950–6840	5.7	1.0
April 14.596	17.496	6300–9250	5.4	1.0
April 15.643	18.543	3870–6890	5.7	1.0
April 16.723	19.623	4280–7400	5.7	1.0
April 17.705	20.605	4000–6900	5.7	1.0
April 19.597	22.497	4200–6900	5.7	1.0
April 21.732	24.632	4000–6810	5.7	1.0
April 22.694	25.594	6210–9250	5.4	1.0
May 1.667	34.567	4530–7100	5.7	1.0
May 17.605	50.505	4000–7030	5.7	1.0
May 18.609	51.509	6120–9210	5.4	1.0

[1]Resolution: 1.5–2.0 pixels

3. Spectrophotometry

Spectrophotometric observations were carried out mostly with the 1-m Zeiss reflector, and in the early phase also with the 2.3-m VBT. Observations were obtained altogether on 16 nights between 1993 April 1 and May 18. The log of observations is presented in Table 2. The observations at 1-m were carried out with the Universal Astronomical Grating Spectrograph coupled with a 250-mm camera and Photometrics CCD system with Thomson-CSF Th7882 chip. A 650 l mm^{-1} grating was used on April 1 and two 150 l mm^{-1} gratings with blue and red blaze angles were used on other nights. The observations at 2.3-m were carried out using Boller & Chivens spectrograph with 150-mm camera and two Astromed CCD systems mentioned in Sect. 2, both with GEC P8603 chip. Both narrow-slit and wide-slit spectra were generally recorded to correct for errors caused by atmospheric dispersion. Feige 34 (Massey et al. 1988; Massey & Gronwall 1990) was used as spectrophotometric standard and star B as comparison. The exceptions to the procedure are as follows. No wide-slit spectra were obtained between April 1 and 8. On April 1 and 3 CD $-32°9927$ (Stone & Baldwin 1983) was used as standard, and on May 1, HD 161817 (Philip & Hayes 1983). Star B was not observed between April 1 and 8, and also on April 19 and May 1.

The reductions were carried out using the RESPECT package at VBO (Prabhu & Anupama 1991). A low-order polynomial fit to the ratio of wide-slit to the narrow-slit spectrum was used for correcting the narrow-slit spectra for the effect of atmospheric dispersion. Corrections were made for the mean differential extinction at VBO before correcting for the instrumental response. The atmospheric absorption bands were evened out using masks prepared from the standard star. The final fluxes were corrected for the zero-point by comparing the synthetic $BVRI$ magnitudes with magnitudes determined from VBO when available, or else, chosen from IAU and e-mail circulars. The spectra were dereddened assuming $E(B-V) = 0.17$. this value agrees with the estimates of $E(B-V) = 0.15 \pm 0.02$ (Wheeler et al. 1993), and $A_v = 0.58 \pm 0.05$ (Lewis et al. 1994) in the literature. Richmond et al. (1994), however, discuss the large uncertaintly in the reddening estimate ranging from $E(B-V) = 0.08$ to 0.32. We discuss the effect of this uncertainty on distance determination by expanding photosphere method in Sect. 4.

3.1. Evolution of the spectrum

Though the spectrum of day 4 is noisy and has a limited range, it was apparent that it was continuous with blue-shifted absorption due to Hα barely discernible. This epoch is close to the first maximum in the light curve. As the photosphere began to recede, the P-Cygni type absorption and emission profiles became apparent on day 6. Prominent among these are Hα and He I λ5876. The Hα line shows a broad absorption with the dip centred at -18730 km s^{-1} and also a narrower absorption at -12890 km s^{-1}. The latter is apparent also on day 4. There are additional dips seen at wavelengths 6470Å on day 4 and 6476Å on day 6. It is not clear whether these are components of Hα or absorption dips of He I λ6678. O I 7774Å line is probably present, on day 6, with the absorption component coinciding with the 7600Å band. At this low resolution, the interstellar Na I D line in our Galaxy and M 81 cluster is seen as a blend at 5893Å.

The spectroscopic evolution to the second maximum is shown in Fig. 1. The emission lines are continuously gaining in strength. Several lines of Fe II are seen shortward of He I λ5876. In particular, multiplets 37 and 38 blend in the range $\lambda\lambda$4549–4629. The peak of this broad feature appears to be de-

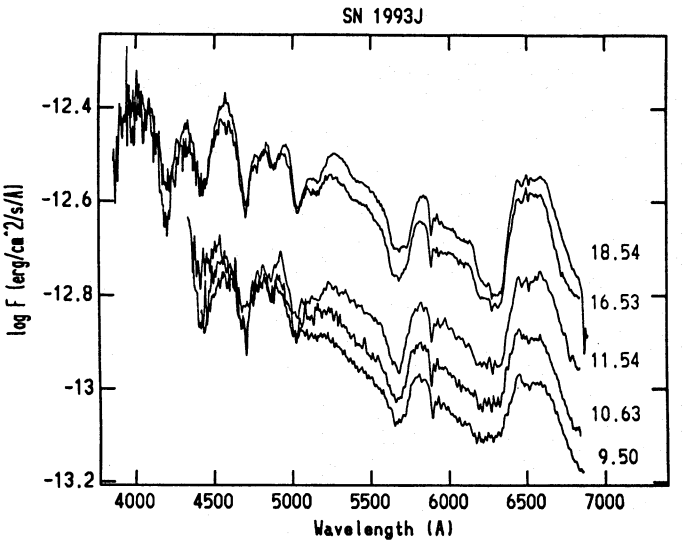

Fig. 1. Spectra of SN 1993J between day 9.50 and 18.54, while the SN brightened to its secondary maximum. Since the signal-to-noise ratio of the first three spectra was poor, they have been smoothed to an effective resolution of 15Å

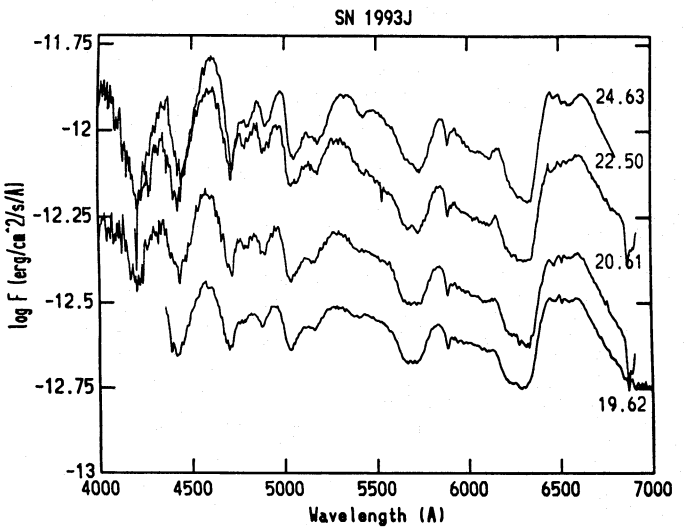

Fig. 2. Spectra of SN 1993J between day 19.62 and 24.63, around the time of secondary maximum. Successive spectra are shifted by 0.2 dex for clarity with the scale on left corresponding to the spectrum of day 19

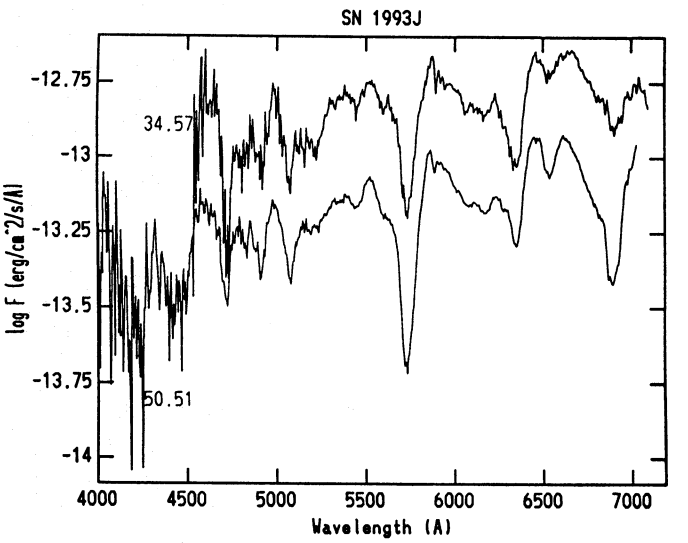

Fig. 3. Spectra of SN 1993J during the decline

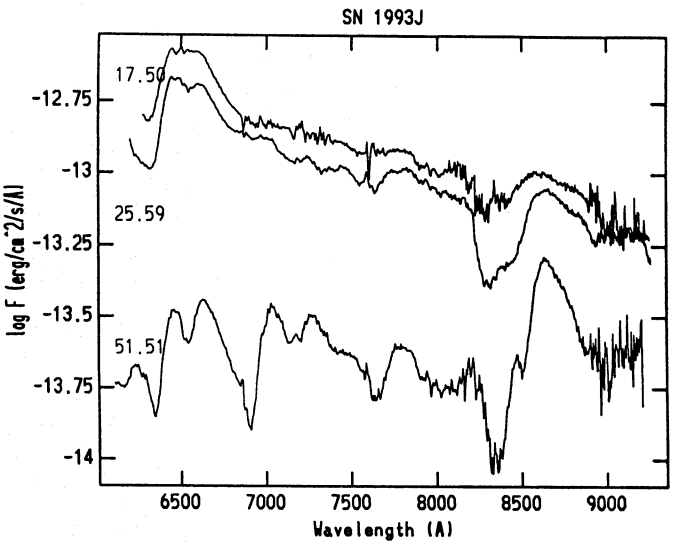

Fig. 4. Spectra of SN 1993J in the red-infrared region between day 17.50 and 51.51, showing a dramatic increase in the strength of lines due to He I, O I, Ca II and Ca II]. Successive spectra are shifted downwards by 0.2 dex for clarity. Note the evidence for N I (1) redward of Ca II infrared triplet in the first two spectra

termined mainly by λ4549 line of multiplet 38. The line-list for synthetic spectra of SN 1987A due to Jeffery & Branch (1990) is useful for identification of observed lines. A comparison with the spectra of Fe II type of novae is particularly helpful since the widths of these lines in novae are intermediate between the normal stars and supernovae, thus affording both the identification and comparison (cf. V443 Scuti 1989: Anupama et al. 1992).

Fe II $\lambda\lambda$4924, 5018 (42) are blended with Hβ; λ5169 (42) is blended with Mg I λ5184 at an effective wavelength of λ5176. Fe II (41, 48, 49) produce a broad blend between $\lambda\lambda$5264–5414. We estimate the peak of this blend to be around λ5300. At later stages, the peak could have been determined largely by the dominant lines of multiplets 48 and 49 around λ5330. Multiplet 55 (λ5535) is blended with the longward wing of the broad λ5300 feature.

Na I D is likely to contribute to He I λ5876. The spectrum on April 15 (18 days since outburst) resembles that of SN 1987A about 11 days from maximum (Dopita 1988). Note that the secondary maximum in SN 1987A occurred between 70–90 days since outburst. Spectra of SN 1987A near secondary maximum had quite strong lines of Sc II $\lambda\lambda$5527, 5658, 6246, 6310 and Ba II λ4554, 6142. These lines are not so prominent in SN 1993J

near second maximum. We conclude that the spectra show primarily the lines due to H, He I, Na I, Mg I, and Fe II.

Though the Hα emission is essentially flat-topped, some structure continues to be visible during the rise to the secondary maximum (see Filippenko et al. 1993, and references therein). There is structure in the absorption profile of Hα as well as He I λ5876. Both these absorption profiles become flat or box-shaped near the secondary maximum. This is probably due to blending with weaker lines which can produce significant changes in line profiles in expanding atmospheres (Jeffery & Branch 1990).

The hydrogen and helium lines show flat-bottom absorption near the secondary maximum (Fig. 2) which begins to turn into a triangular profile by day 24. The double-peaked structure of Hα+He I emissions become more pronounced by this time.

The spectra during the decline are shown in Fig. 3. The linear decline begins around day 44. The absorption features of strong lines become sharp by this time. The double structure around Hα can now be easily understood to be due to the superposition of the P-Cygni profile of He I λ6678 (Filippenko et al. 1993). He I λ7065 is quite strong by this time, and He I λ5876 gains in strength. The features blended with the fading Hβ are probably due to He I $\lambda\lambda$4922, 5016 rather than Fe II. The absorption due to Fe II λ5535 has become rather strong and its emission component is also discernible. This feature may have significant contributions due to Sc II λ5527 as well as the blue-shifted emission of O I λ5577 which becomes stronger a little later (Lewis et al. 1994).

The red spectra on days 17, 25 and 51 are shown in Fig. 4. The most dramatic changes here are in the near-infrared triplet of Ca II and O I λ7774 both of which steadily gain in strength. There is excess emission to the redward of calcium triplet during the early phases which is very likely due to N I (1). There is also an indication of N I (2) near λ8200 during this phase. Similar enhancement of N I was seen also in SN 1987A (Ashoka et al. 1987). The increasing strength of He I $\lambda\lambda$6678, 7065 is clearly evident in the figure. He I λ7281 also appears around day 28, and Ca II] $\lambda\lambda$7291, 7324 by day 51.

The absorptions dips due to Ba II λ6142 and Sc II λ6246 are evident clearly on day 50. The dips can be traced back with some difficulty till day 22. Ba II λ5854 is probably blended with He I D emission, whereas Sc II λ5658 absorption appears just blueward of the point where the absorption due to He I D reaches the continuum. The implied velocities of these lines are however, much lower than indicated by even the Fe II lines. These lines are generally expected in the helium core where the elements are synthesised by s-process. They were much stronger in the spectra of SN 1987A and suggested mixing between the envelope and core (see Dopita 1988). The late appearance and low strength of these lines in SN 1993J suggest that there was no significant mixing.

3.2. Evolution of absorption velocities

The large expansion velocity of the supernova ejecta and consequent line broadening results in severe line blending. However, a few individual lines or blends can be easily identified. We have measured the expansion velocity as inferred from the absorption minima of lines Hα, Hβ, Hγ, He I + Na I D, Fe II $\lambda\lambda$4549, 4924, 5018, 5300, and Mg I + Fe II λ5176. In addition, O I λ7774, and Ca II $\lambda\lambda$8542, 8662 lines could be measured on some of the near-infrared spectra and the lines He I $\lambda\lambda$6678, 7065, Ba II λ6142 and Sc II λ6246 during the late phases. All the measured velocities are listed in Table 3 and plotted in Fig. 5. We did not measure weak lines in the poor quality spectra of April 6, 7 and 8. N I λ8215 was probably present on April 14 (8710 km s^{-1}). He I λ4922, 5016 contribute to Fe II λ4924, 5018 at late stages. Some of the scatter in the inferred velocities is due to inaccurate mean positions assumed for lines which may vary continuously as the contributions to the blends vary with time. We did not measure the velocity of He I λ7281 because of possible contamination due to Ca II]. The strong lines such as Hα and Na I D show broad absorption dips up to the second maximum in the light curve. The absorption dip in such cases is defined as the centre of the broad absorption rather than a local dip in this band since it was noticed whenever we had good signal-to-noise (> 70 in the absorption dips) that the local dip keeps migrating probably due to structure in the atmosphere.

All the absorption velocities decrease with time implying that the velocities in the expanding atmosphere decrease inward in the mass coordinate system. The inferred velocities are the highest for Hα, and reduce for higher Balmer lines and lines due to He I, and are the lowest for metallic lines. Since the optical thickness in Balmer and He I lines is high, these lines are formed in the outermost layers which explains the behaviour just as in the case of SN 1987A (Dopita 1988). The metallic lines are formed close to the photosphere. The lines of Ba II and Sc II which develop during the decline from the second maximum give the lowest velocities. The low velocity of Fe II 5535 line at later epochs is probably due to the contribution of Sc II λ5527. The Fe II line at 5300Å also has lower velocities during later epochs; this is likely due to a shift in the mean wavelength of the line to the red due to a variation in the relative intensities of contributors to the blend.

4. Evolution of the photosphere

As the supernova envelope expands, the continuum optical depth decreases causing the photosphere to move inwards. This provides an opportunity to probe the inner layers of the ejecta as time progresses. It is generally assumed that the supernova ejecta expand homologously. The radius of a shell at time t would hence be $r_0 + vt$ where r_0 is the radius of the shell before explosion (which could be neglected for times greater than a few days for progenitor radii a few hundred $R_\odot$), and v is the expansion velocity of the layer which is independent of time. If the photospheric radius varies as t^m, the photospheric velocity is implied to vary as $t^{(m-1)}$. If the density in the envelope varies as $\rho \propto r^{-n}$, one obtains a time variation of velocity as $t^{-2/(n-1)}$. The two exponents are hence related as $n = (m-3)/(m-1)$ (see Jeffery & Branch 1990). The observations of SN Ia show that the observed value of n lies in the range 5–12 with the most favoured value of 7 (Branch, Drucker & Jeffery 1973; see also

Table 3. SN 1993J: Absorption velocities.

Day	Hγ λ4340	Fe II λ4549	Hβ λ4861	Fe II λ4924	Fe II λ5018	Fe II+Mg I λ5176	Fe II λ5300	Fe II λ5535
9.50			10360					
10.63			9810					
11.54			9990					
16.53	9810	8090	9250	8460	8180	7990	7860	
18.54	9260	7830	9280	7880	7590	7590	7750	
19.62			9420	8280	7950	7930	7610	7580
20.61	9190	7560	9090	7610	7470	7570	7920	7370
22.50		8090	9000	7370	7290	7010	7180	5900
24.63	8640	6670	8450	7170	6570	6810	6390	5960
34.57			8390	6640	6300	6000	4400	4500
50.51			8520	5970	5910	5390	4070	4370

Day	He I λ5876	Ba II λ6142	Sc II λ6246	Hα λ6563	He I λ6678	He I λ7065	O I λ7774	Ca II λ8542	Ca II λ8662
6.57	11830			18730				9970	
9.50	11070			16900					
10.63	10870			13930					
11.54	10100			14160					
16.53	9690			13610					
17.50							8500	8700	8830
18.54	9440			13660					
19.62	9900			13930					
20.61	9590		7440	12920					
22.50	9290	5340	6270	12700					
24.63	7550	4780	6100	12270					
25.59				12330				8360	8460
34.57	6950	3840	4930	9960	6510	6660			
50.51	7040	3370	3120	9790	6290	7040			
51.51				9620	6100	6790	5210	6770	5490

Prabhu & Krishnamurthi 1990). In the case of supernovae of other types, it is not necessary that the same exponent may hold in all the zones inside the progenitor. For SN 1987A, Jeffery & Branch (1990) derive a value of $n = 4.5$ during the rise to the second maximum. The exponent began to decrease soon after the maximum.

Since the photometric determinations yield angular measures and spectroscopy yields linear velocities, a comparison of the two yields an estimate of the distance to the supernova. This is the essence of 'expanding photosphere method' used on supernovae (Branch & Patchett 1973; Kirshner & Kwan 1974) as a variant of the Baade-Wesselink method on Cepheids, which itself is derived from a more general suggestion due to Baade. An application of the method to supernovae in nearby galaxies with distances known fairly accurately would help increase our confidence in the application of the method to more distant galaxies (cf. Schmidt-Kaler 1991 on SN 1987A, and Schimdt et al. (1994) on determination of H_0).

4.1. Photometric estimates of angular radius and velocity of photosphere

The luminosity, temperature and radius of the photosphere can be estimated from a blackbody fit to the observed magnitudes (e.g. Ray et al. 1993), or by comparing the colours with a supergiant (Ashoka et al. 1987). While yielding fairly good estimates for the total luminosity, both these methods are beset with problems of contribution due to emission and absorption components (Branch 1979). A better alternative is to compare the actual continuum derived from spectrophotometry with blackbody spectrum. The problem with this alternative is that the errors in instrumental response correction and limited range of observed spectra introduce large error in temperature and hence in the angular radius. The best estimates can be arrived at only by comparison of UV-optical-IR spectra with theoretical model spectra (see Jeffery & Branch 1990; Baron et al. 1994).

We have determined photospheric radii from broadband photometry. The optical data alone are sufficient, in principle, to determine the colour temperature of the optical photosphere. The U band and near-ultraviolet spectrum are known to contain

lower flux compared to blackbody fit to the optical region (Jeffery et al. 1994), because of line-blanketing. We find that the B band does not suffer appreciably in the case of SN 1993J, at least until the rise to the second maximum. The $B-V$ and $V-R$ colours, however, do not give a consistent value for temperature, the former yielding a higher temperature. The difference reduces with time, though. The inclusion of JHK bands helps in constraining the blackbody curve better. We hence use these bands after correcting for interstellar extinction and for net emission contribution due to superposed P-Cygni profiles.

The correction factor for the net contribution due to lines to the broadband magnitudes was estimated from the spectrophotometric data by extracting synthetic $BVRI$ magnitudes from continuum-reduced spectra. These corrections, which are in the form of (total magnitude − continuum magnitude), appear to vary smoothly between day 6 and 51 and are negligible at early epochs when the absorption component is equal to the emission component as expected for purely scattering atmosphere. The following formal fits were obtained to the data, with standard errors of 0.03 – 0.06:

$$\Delta B = -0.135 + 0.147 t_{\rm d}^{\ 1/3}; \qquad t_{\rm d} > 1; \tag{1}$$

$$\Delta V = -0.324 + 0.170 t_{\rm d}^{\ 1/3}; \qquad t_{\rm d} > 7; \tag{2}$$

$$\Delta R = -0.387 + 0.181 t_{\rm d}^{\ 1/3}; \qquad t_{\rm d} > 10; \tag{3}$$

$$\Delta I = -0.448 + 0.157 t_{\rm d}^{\ 1/3}; \qquad t_{\rm d} > 23. \tag{4}$$

The epoch of onset given at the end of the fits is the time when the fit implies vanishing correction. The correction becomes significant in the blue region very quickly, and is not very significant in the infrared during the period of our observations. We have not corrected JHK magnitudes for line emission since we did not have spectra in this region. Infrared spectra of Swartz et al. (1993) show the important contributions due to Paschen α, β, Bracket γ, He I 1.08, 2.16 μm and Fe II 1.64 μm. Since the continuum flux peaks in the optical, the small corrections required for these lines in the infrared will not have significant effect on the parameters determined by ignoring them.

We supplement our BVR photometry with I band of Schmidt et al. (1993) and JHK photometry of Lawrence et al. (1993) and Romanishin (1993). We found that the last two sources mutually agree and a few other measures available in literature differ systematically from these. We correct our R values for the systematic error of 0.05 mag explained in the earlier section. We also supplement this set with $BVRI$ photometry of day 6.3 based on Schmidt et al. since JHK photometry is available at this epoch. Similarly, we use the data of Lewis et al. (1994) whenever the full set of $BVRI$ is available and interpolate for JHK from Lawrence et al. . We use the emission-line corrections listed above with a slight extrapolation to day 58. These corrections bring the $BVRI$ colours closer to the blackbody colours compared to the uncorrected ones (cf. Richmond et al. 1994) showing that a major cause of the apparent departure from blackbody is the presence of emission lines.

There appears to be considerable uncertainty in the reddening estimates for SN 1993J. While the UV continuum and X-ray observations suggest a low value for reddening, the interstellar absorption lines and diffuse bands indicate moderate reddening (Richmond et al. 1994; Benetti et al. 1994). We correct our data for reddening assuming two extreme values suggested by Richmond et al. : $E(B-V) = 0.08$ and 0.32. After these corrections, the blackbody fits were obtained using the NFIT1D task of STSDAS[2], keeping the reference wavelength fixed at 6000Å, and varying the temperature and amplitude. The results are presented in Table 4.

Table 4. Blackbody fits to corrected $BVRIJHK$ magnitudes.

Day	$E(B-V)=0.08$		$E(B-V)=0.32$		Notes
Day	$T_{\rm eff}$	θ	$T_{\rm eff}$	θ	
	K	10^{-10} rad	K	10^{-10} rad	
6.30	7790	0.629	11010	0.525	
6.89	7430	0.639	10380	0.530	*
7.91	7110	0.666	9760	0.555	*
8.89	6980	0.701	9480	0.589	*
9.89	6910	0.728	9310	0.617	*
10.96	6910	0.750	9310	0.635	*
11.88	7050	0.786	9550	0.667	*
13.01	7090	0.810	9510	0.700	*
13.87	6940	0.889	9250	0.767	*
17.58	6880	1.012	9020	0.894	
18.57	7010	1.003	9280	0.881	
19.58	6830	1.068	8910	0.947	
20.55	6430	1.182	8160	1.072	
21.52	6630	1.127	8560	1.004	
22.52	6210	1.253	7800	1.140	
24.51	5800	1.384	7090	1.286	
24.86	5830	1.363	7150	1.258	*
25.49	5520	1.489	6610	1.414	
26.81	5390	1.490	6430	1.411	*
27.50	5310	1.479	6310	1.403	
27.79	5330	1.447	6320	1.383	*
28.81	5010	1.571	5920	1.530	*
30.81	4880	1.613	5590	1.603	*
31.77	4780	1.636	5440	1.637	*
33.78	4710	1.609	5340	1.612	*
38.70	4590	1.521	5190	1.517	*
47.80	4590	1.313	5210	1.309	*
48.80	4580	1.298	5200	1.290	*
55.78	4640	1.163	5260	1.160	*
57.81	4630	1.137	5260	1.129	*
58.78	4670	1.099	5330	1.085	*

* $BVRI$ data from Lewis et al. (1994)

Increasing the reddening correction has the effect of increasing the temperature of the fit and reducing the radius. The increase in temperature for moderate reddening compared to low reddening is 40% in early days and reduces to 20% during the secondary maximum and 15% during the later phases. The effect on radius is relatively lower, ranging from 20% in the early

[2] The Space Telescope Science Data Analysis System (STSDAS) is distributed by the Space Telescope Science Institute.

days to 5% near second maximum and < 1% durint the later phases.

The temperatures derived above are lower than the values derived by Richmond et al. (1994) for the two cases using $BVRI$ data alone and without correcting for the emission lines. They are, on the other hand, larger than the estimates of Ray et al. (1993) using the $UBVRIJHK$ photometry with no corrections for reddening or line flux. The estimates of Lewis et al. (1994) using $UBVRIJHK$ photometry and an extinction of $A_v = 0.58$ lie between our two estimates. Our estimates of radii are slightly larger than those of Lewis et al. but lower than those of Ray, Singh & Sutaria. The radii determined from spectroscopic models by Baron et al. (1993) on April 7 (day 10) and 13 (day 16) are slightly larger than the values derived here.

We use the photometric angular radii to derive the expansion velocities at an assumed distance of 3.6 Mpc. The derived velocities are fairly constant during the well-observed period between days 17 and 27 within the errors of blackbody fits at $\log v = 3.855 \pm 0.015$ and 3.814 ± 0.023 for the low and moderate reddening cases, v being the expansion velocity in km s^{-1} . The constant velocity implies either a very steep density drop, or a discontinuity in the structure. Assuming the latter, we make the following fit for the period 6.3 and 21.5,

$$\log v = 4.4707 - 0.4862 \log t_d\,, \qquad E(B-V) = 0.08, \quad (5)$$

$$\log v = 4.3348 - 0.4215 \log t_d\,, \qquad E(B-V) = 0.32. \quad (6)$$

The first fit implies an exponent $n = 5.1$ and the second 5.8. These values should be compared with the value of 4.5 during the rise to the second maximum for SN 1987A (Jeffery & Branch 1990), and the mean value of 7 for SN Ia during the post-maximum phase (Branch et al. 1973). Between days 30.8 and 58.8 we similarly obtain

$$\log v = 6.2413 - 1.6090 \log t_d\,, \qquad E(B-V) = 0.08, \quad (7)$$

$$\log v = 6.2553 - 1.6187 \log t_d\,, \qquad E(B-V) = 0.32, \quad (8)$$

implying $n = 2.2$ for either value of reddening. In the case of SN 1987A the exponent had similarly reduced to 2 (Jeffery & Branch 1990).

The velocity estimates based on photometry are plotted in Fig. 5 together with the observed velocities. Also plotted in the figure are the photometric velocities derived using the blackbody fits published by Lewis et al. (1994) and Richmond et al. (1994) after scaling them to the distance of 3.6 Mpc adopted by us. It is evident that the radii obtained by using $UBVRI$ alone are underestimated compared to the values obtained by including JHK magnitudes. The exclusion of U band and correcting the spectrum for emission flux has the effect of increasing the radii slightly.

4.2. Distance estimate by expanding photosphere method

It is apparent from Fig. 5 that the photometric velocities agree with the spectroscopic velocities of the weakest lines if the interstellar extinction is $E(B-V) = 0.08$. The estimates for moderate reddening fall short of observed velocities and a good fit

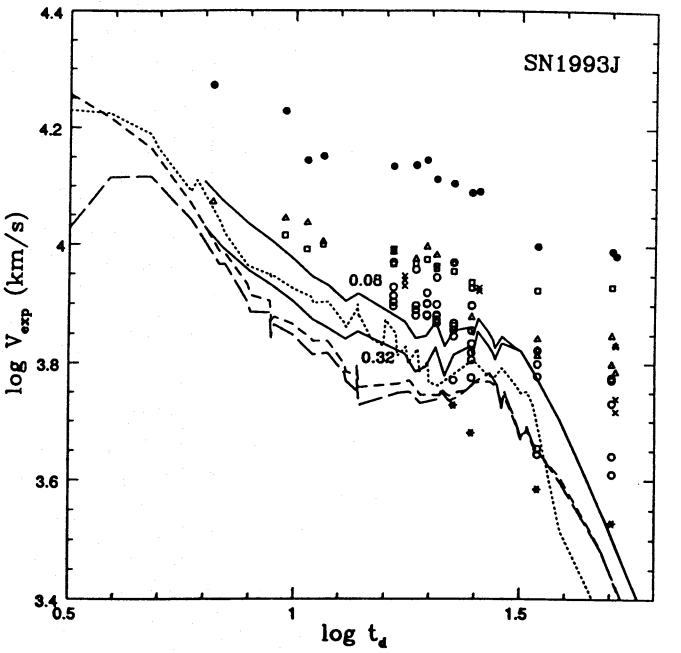

Fig. 5. Variation of velocities of different absorption lines observed in the spectra of SN 1993J as a function of time since outburst. Filled circles: Hα; open squares: Hβ, Hγ; open triangles: He I lines; open circles: Fe II lines; crosses: Ca II and O I lines; stars: Ba II and Sc II lines. The continuous lines denote photometric velocities derived from the radii estimated by us for the two values of $E(B-V)$ as marked. The dotted line is based on radii determined by Lewis et al. (1994) for an $A_v = 0.58$. The short-dashed lines and the long-dashed lines are based on the blackbody fits of Richmond et al. (1994) for $E(B-V) = 0.08$ and 0.32 respectively

requires a distance of 4.0 Mpc. We ignore here the systemic velocity of SN 1993J which is estimated as -119 or -135 km s^{-1} based on the observations of interstellar matter in the vicinity (Vladilo et al. 19933). We have also not reduced our velocities to Sun, the corrections being of much smaller magnitude. These corrections together add up to less than 5% of the observed velocities and are comparable to uncertainties in the estimates of velocity dips of blended profiles.

An uncertainty is introduced in the expanding photosphere method due to the fact that the photosphere may not exactly behave like a blackbody. There can be some reduction of flux due to the photons lost by being scattered inwards (measured by the dilution factor ζ). On the other hand, there can be excess emission from an extended photosphere. The former dominates during the early period and the latter during the later phases, suggesting that there could be a period in between when the two effects cancel out each other (Jeffery & Branch 1990). Thirdly, the method assumes that the supernova envelope is spherical. Any asymmetry in the actual situation would demand a correction factor that depends on the viewing angle (Shapiro & Sutherland 1982). Based on polarimetric observations of SN 1987A, it was suggested by Schmidt-Kaler (1991) that the correction factor would either be 0.94 or 1.05 depending on whether the photosphere is oblate or prolate. The spectropolarimetric obser-

vations of Trammell et al. (1993) suggest that the asymmetry could be slightly larger in the case of SN 1993J.

In the case of SN 1987A, the flux reduction reduced the photometric radius to just half of photospheric radius on day 2 since the outburst. Between days 6 and 15 the discrepancy rapidly decreased. Subsequently the flux deficit was apparently compensated by atmospheric emission effects (Jeffery & Branch 1990). If one assumes a flux deficit of 20% in the case of SN 1993J around day 10 and 10% near secondary maximum, the distance of 3.6 Mpc is compatible even with a reddening of $E(B-V) = 0.32$. The atmosphere of SN 1993J had much lower mass compared to SN 1987A and hence the atmospheric emission may not have caught up fully with the flux deficit until the secondary maximum.

Since the extinction correction reduces the estimated radii and correction for flux deficit increases them, we can obtain the limits on distance estimate with extreme assumptions. Detailed models for SN II yield a value of $\zeta \sim 0.4$ for $T_{\rm eff} \sim 6000$ K. The value of ζ approaches unity as the temperature decreases (Schmidt et al. 1994; note that their distance correction factor ζ is the square-root of the dilution factor or flux deficit factor used here). Since the envelope of SN 1993J is less massive, the value of ζ is likely to be closer to unity. For the purpose of putting stringent limits on distance, we will assume the reddening limits noted above and limits of $\zeta = 0$ and 0.4. In the case of low reddening and moderate flux deficit, the best fit distance is 2.2 Mpc and in the case of moderate reddening and no flux deficit, the distance is 5.1 Mpc. Thus, in the absence of accurate knowledge of the two, the expanding photosphere method is able to provide the distance to SN1993J to an accuracy of about 40%. This is an encouraging result since the accuracy of the method is independent of distance since similar photometric and spectroscopic accuracies can be attained for much larger distances. Detailed atmospheric models should be able to reduce the uncertainty in the flux deficit considerably. Also the reddening correction and flux deficit correction work in opposite directions. Schmidt et al. (1994), find that an accuracy of 10% can be achieved using EPM method for standard type II SN together with atmospheric models.

5. Conclusions

The spectroscopic data presented here during the period when SN 1993J brightened from the dip following the initial decline to a little after the secondary maximum, show that the transition from type II to type Ib took place soon after the secondary maximum when the photosphere had receded into the helium core. There are strong indications that there was no mixing of the *s*-process elements with the atmosphere. The enhancement of N I lines is noticed during the rise to second maximum just as in the case of SN 1987A. The density law in the atmosphere is slightly steeper than for SN 1987A during the rise to the second maximum, but is comparable during the subsequent decline. The expanding photosphere method yields a distance consistent with other independent methods. The distance estimates obtained using extreme values of reddening and atmospheric dilution factor depart from the HST Cepheid determination by $< 40\%$.

Acknowledgements. We are grateful to G. C. Anupama, Gopal-Krishna, S. K. Jain and M. Parthasarathy for making available a part of their observing time at VBO. We also thank the assistants at both the telescopes for help, and on occasion, for obtaining the data. The paper has benefitted a great deal by our interaction with G. de Vaucouleurs, J. C. Wheeler, Alak Ray and Firoza Sutaria. We also thank the referee, E. Cappellaro, for useful comments.

References

Anupama G.C., Duerbeck H.W., Prabhu T.P., Jain S.K. 1992, A&A 263, 87
Anupama G.C., Kembhavi A.K., Prabhu T.P., Singh K.P., Bhat P.N. 1994, A&AS 103, 315
Ashoka B.N., Anupama G.C., Prabhu T.P. et al. 1987, JA&A 8, 195
Baron E., Hauschildt P.H., Branch D. et al. 1993, ApJ 416, L21
Baron E., Hauschildt P.H., Branch, D. 1994, Preprint
Bartel N., Bletenholz M.F., Rupen M.P. et al. 1994, Nature, 368, 610
Benetti S., Patat F., Turatto M., Contarini G., Gratton R., Capellaro E. 1994, A&A 285, L13
Benston P.J., Herbst W., Salzer J.J. et al. 1994, AJ 107, 1453
Branch D. 1979, MNRAS 186, 609
Branch D., Patchett B. 1973, MNRAS 161, L71
Branch D., Drucker W., Jeffery D.J. 1988, ApJ 330, L117
Corwin H.C. 1993, IAU Circ. 5742
Dopita M.A. 1988, Sp Sci Rev 46, 225
Filippenko A.V. 1988, AJ 96, 1941
Filippenko A.V. 1991, in Ray A., Velusamy T., eds, Supernovae and Stellar Evolution. World Scientific, Singapore, p.34
Filippenko A.V., Matheson T., Ho L.C., 1993, ApJ 45, L103
Freedman W.L., Hughes S.M., Madore B.F. et al. 1994, preprint
Harkness R.P., Wheeler J.C. 1990, in Petschek A.G., ed., Supernovae. Springer-Verlag, New York, p.1
Höflich P., Langer N., Duschinger M. 1993, A&A 275, L29
Jeffery D.J., Branch D. 1990, in Wheeler J.C., Piran T., Weinberg S., eds, Supernovae. World Scientific, Singapore, p.149
Jeffery D.J., Kirshner R.P., Challis P.M. et al. 1994, ApJ 421, L27
Kirshner R.P., Kwan J. 1974, ApJ 193, 27
Lawrence G.F., Paulson A., Mason C., Butenhoff C., Gehrz R.D. 1993, IAU Circ. 5884
Lewis J.R., Walton N.A., Meikle W.P.S. et al. 1994, MNRAS 266, L27
Massey D., Gronwall 1990, ApJ 358, 344
Massey D., Strobel K., Barnes J.V., Anderson W. 1988, ApJ 328, 315
Mayya Y.D. 1993, PhD Thesis, Indian Institute of Science, Bangalore
Nomoto K., Suzuki T., Shigeyama T. et al. 1993, Nature 364, 507
Philip A.G.D., Hayes D.S. 1983, ApJ 53, 571
Podsiadlowski Ph., Hsu J.J.L., Joss P.C., Ross R.R. 1993, Nature 364, 509
Prabhu T.P. 1994, Proc. 8th IAU Asia-Pacific Regional Meeting: JA&A (in press)
Prabhu T.P., Anupama G.C. 1991, Bull astr Soc India 19, 97
Prabhu T.P., Krishnamurthi A. 1990, A&A 232, 75
Ray A.K., Singh K.P., Sutaria F.K. 1993, JA&A 14, 53
Richmond M.W., Treffers R.R., Filippenko A.V. et al. 1994, AJ 107, 1022
Ripero J. 1993, IAU Circ. 5731
Romanishin W. 1993, IAU Circ. 5773

Schmidt B.P., Kirshner R.P., Eastman R.G. et al. 1993, Nature 364, 600
Schmidt B.P., Kirshner R.P., Eastman R.G. et al. 1994, ApJ 432 (in press).
Schmidt-Kaler T. 1991, in Danziger I.J., Kjär K., eds, Supernova 1987A and other Supernovae. ESO, Munich, p.311
Shapiro P.R., Sutherland P.G. 1982, ApJ 263, 902
Stone R.P.S., Baldwin J.A. 1983, MNRAS 204, 347
Swartz D.A., Clochiatti A., Benjamin R., Lester D.F., Wheeler J.C. 1993, Nature 365, 232
Trammell S.R., Hines D.C., Wheeler J.C. 1993, ApJ 414, L21
van Driel W., Yoshida, S., Nakada, Y. et al. 1993, PASJ 45, L59
Vladilo G., Centurión M., de Boer K.S. et al. 1993, A&A 280, L11
Wheeler J.C., Filippenko A.V. 1993, Univ. Texas Preprint
Wheeler J.C. et al. 1993, ApJ 417, L71
Woosley S.E. 1991, in Woosley S.E., ed., Supernovae. Springer-Verlag, p.202
Woosley S.E., Pinto P.A., Martin P.G., Weaver T.A. 1987, ApJ 318,664
Woosley S.E., Eastman R.G., Weaver T.A. 1994, preprint
Woosley S.E., Eastman R.G., Weaver T.A., Pinto P.A. 1994, preprint

This article was processed by the author using Springer-Verlag LaTeX A&A style file version 3.